LCDA Moments of Mesons from Local and Non-local Operators

Speaker: Ji-Hao Wang
Institute of Theoretical Physics， Chinese Academy of Sciences

LaMET 2025
Oct. 10th . 2025

Motivation and Background

Light-cone distribution amplitudes (LCDAs) plays an important role in the hardon hard exclusive reactions.

- Semi-leptonic B meson decays
- Hard exclusive meson production
- Pion-photon transition form factor
- …

The LCDA is defined through matrix elements of non-local operators

$$i f_M (P \cdot n) \phi(x) = \int \frac{d\xi^-}{2\pi} e^{-ixP^+\xi^-} \langle \Omega | \bar{\psi}_1(0) \not{n} \Gamma U(0, \xi^-) \psi_2(\xi^-) | M(\vec{p}) \rangle,$$

There are two ways to extract information of LCDA on lattice:

1. Calculate moments using twist-2 local operators on lattice and reconstruct the LCDA.
2. Calculate the quasi-DA correlators on the lattice and match it to the LCDA through large-momentum effective theory(LaMET).

In previous work, there are some deviations between the moments obtained by LaMET and twist-2 local operators. In this work we systematically investigate moment calculations using various methods on identical ensembles

Moments from twist-2 local operator

The moments of LCDA can be expressed by twist-2 local operator:

$$\mathcal{N}_{(\mu\mu_1\ldots\mu_n)}\left[\int_0^1 dx(2x-1)^n\phi_M(x,\mu^2)\right] = if_M\langle\Omega|\bar{q}_2(x)\Gamma\gamma_{(\mu}\overleftrightarrow{D}_{\mu_1}\ldots\overleftrightarrow{D}_{\mu_n)}q_1(x)|M(\vec{p})\rangle$$

kinematical factor

Mellin moments
$\langle\xi^n\rangle_M(\mu^2)$
where $\xi = 2x-1$

Symmetry traceless operator

In this work, we calculate the first moments and second moments

- First moments:

$$\mathcal{O}^-_{\rho\mu}(x) = \bar{q}_2(x)\left[\overleftarrow{D}_{(\mu} - \overrightarrow{D}_{(\mu}\right]\gamma_{\rho)}\Gamma q_1(x)\,, \qquad \langle\Omega|\mathcal{O}^-_{\rho\mu}|M(\vec{p})\rangle = if_M\mathcal{N}_{(\rho\mu)}\langle\xi\rangle$$

- Second moments:

$$\mathcal{O}^\pm_{\rho\mu\nu}(x) = \bar{q}_2(x)\left[\overleftarrow{D}_{(\mu}\overleftarrow{D}_{\nu} \pm 2\overleftarrow{D}_{(\mu}\overrightarrow{D}_{\nu} + \overrightarrow{D}_{(\mu}\overrightarrow{D}_{\nu}\right]\gamma_{\rho)}\Gamma q_1(x)\,, \qquad \langle\Omega|\mathcal{O}^-_{\rho\mu\nu}|M(\vec{p})\rangle = if_M\mathcal{N}_{(\rho\mu\nu)}\langle\xi^2\rangle$$

$$\langle\Omega|\mathcal{O}^+_{\rho\mu\nu}|M(\vec{p})\rangle = if_M\mathcal{N}_{(\rho\mu\nu)}\langle 1^2\rangle$$

For pseudo meson the $\Gamma = \gamma_5$, for vector meson the $\Gamma = I$ or γ_μ

Extract moments

Taking the pseudo-scalar meson as an example, we can use these two ratios to obtain the second moments:

$$R^{\pm}_{2,a_1} = -\frac{1}{3}\sum_{i\neq j}^{3}\frac{1}{p_i p_j}\frac{\sum_{\vec{x}} e^{i\vec{p}\cdot\vec{x}}\langle \mathcal{O}^{\pm}_{4ij}(\vec{x},t)P(\vec{0},0)\rangle}{\sum_{\vec{x}} e^{i\vec{p}\cdot\vec{x}}\left\langle A_4(\vec{x},t)P\left(\vec{0},0\right)\right\rangle} \qquad R^{\pm}_{2,a_2} = -\frac{1}{3}\sum_{i=1}^{3}\frac{p_i}{p_1p_2p_3}\frac{\sum_{\vec{x}} e^{i\vec{p}\cdot\vec{x}}\langle \mathcal{O}^{\pm}_{123}(\vec{x},t)P(\vec{0},0)\rangle}{\sum_{\vec{x}} e^{i\vec{p}\cdot\vec{x}}\langle A_i(\vec{x},t)P(\vec{0},0)\rangle}$$

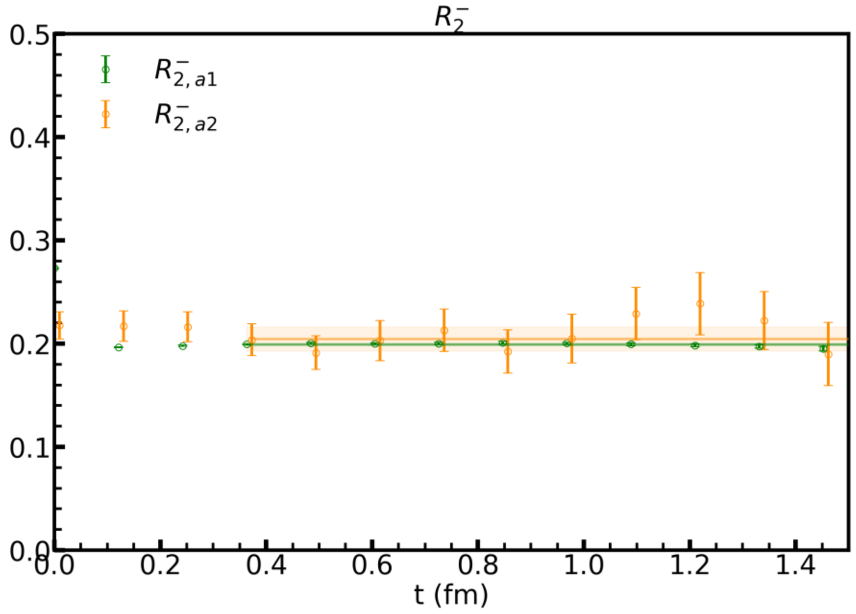

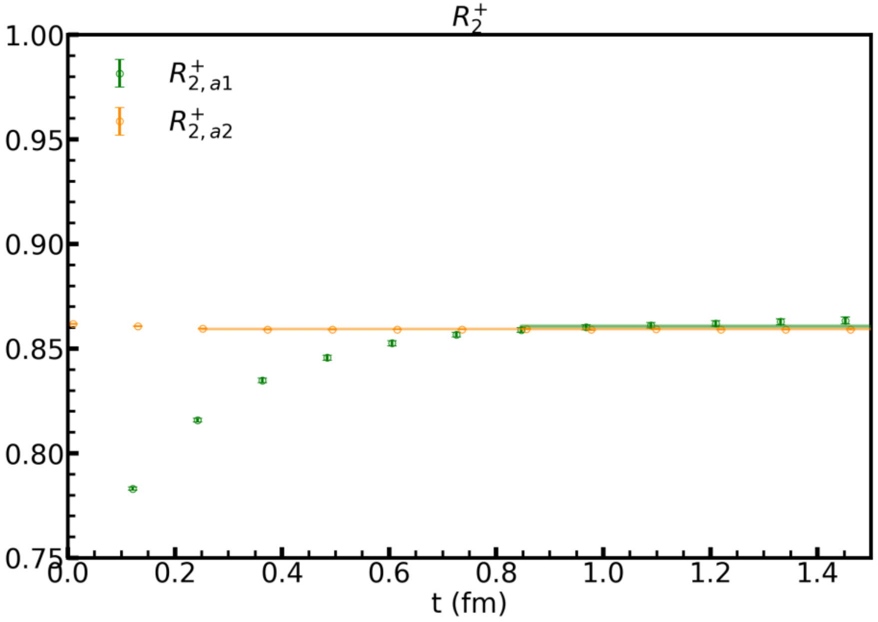

The $R^{\pm}_{2,a1(a2)}$ for the kaon on the ensemble with a=0.121fm and physical pion mass shows consistency between the two channels. However, the excited-state contamination and the behavior of the statistical errors differ between them.

Simulation Setup

Ensembles	a (fm)	$L^3 \times T$	$m_\pi^{\rm v}$	$m_{\eta_s}^{\rm v}$	$m_\pi^{\rm sea}$	$m_{\eta_s}^{\rm sea}$	$N_{\rm conf} \times N_{\rm tsrc} \times N_{\rm multi\text{-}src}$
a04m310	0.0425(5)	$64^3 \times 192$	300	636	315	693	$187 \times 4 \times 2$
a06m310	0.0574(5)	$48^3 \times 144$	322	656	329	725	$83 \times 4 \times 4$
			162	718			$176 \times 4 \times 2$
a09m310	0.0882(7)	$32^3 \times 96$	313	647	316	697	$129 \times 6 \times 2$
			152	690			$129 \times 12 \times 2$
a12m310	0.1213(9)	$24^3 \times 64$	310	612	305	676	$200 \times 2 \times 2$
			190	659			$200 \times 8 \times 2$
a12m220S	0.1213(9)	$24^3 \times 64$	222		220	675	$86 \times 8 \times 2$
a12m220	0.1213(9)	$32^3 \times 64$	225		220	675	$85 \times 8 \times 2$
a12m130	0.1213(9)	$48^3 \times 64$	131	679	132	675	$165 \times 32 \times 2$

Our calculation use four gauge ensembles generated by the MILC collaborationwith 2+1+1 flavors Highly Improved Staggered Quarks(HISQ). We use the 1-step HYP-smeared clover fermion for the valence quark, with several light and strange quark masses on given ensemble

Extrapolation for second moments

The global fit ansatz :

$$\langle\xi^2\rangle_M(m^{\mathrm{v,sea}}_{\pi,\eta_s}, a, 1/L) = \langle\xi^2\rangle_0[1+\delta(c^{(2)}_{1/2,M}, a, 1/L)] + \sum_{X=\mathrm{v,sea}}[c_3^{(2),X}\bar{m}_q^X + n_M c_4^{(2),X}\delta m_q^X],$$

Where $\delta(c_{1/2/3}, a, 1/L) = c_1\bar{\alpha}_s\Lambda_\chi a + c_2\Lambda_\chi^2 a^2$, $\bar{\alpha}_s \equiv -\frac{4}{3}\ln u_0$ and $\Lambda_\chi = 1\,\mathrm{GeV}$

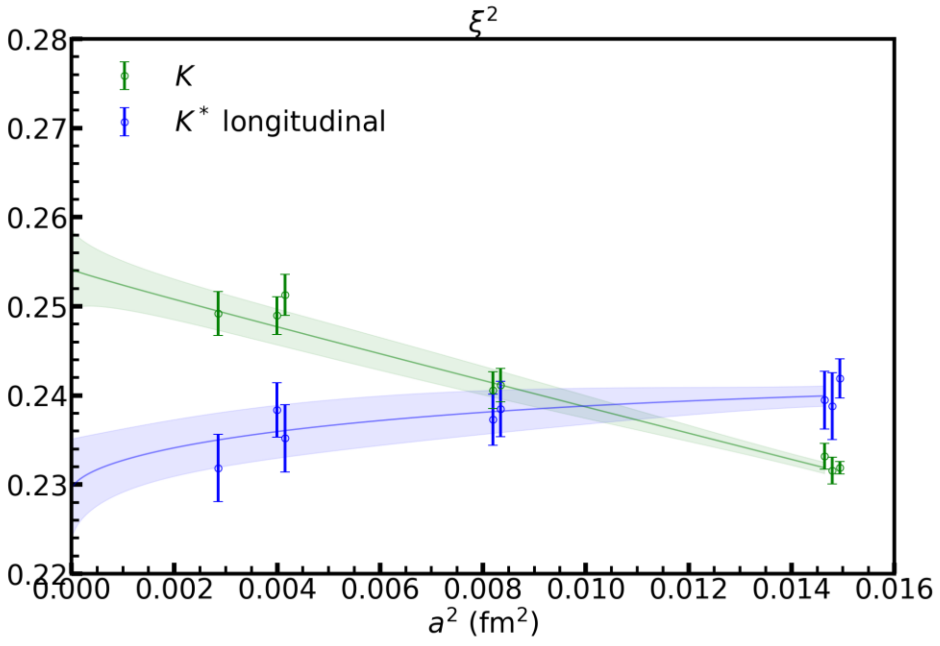

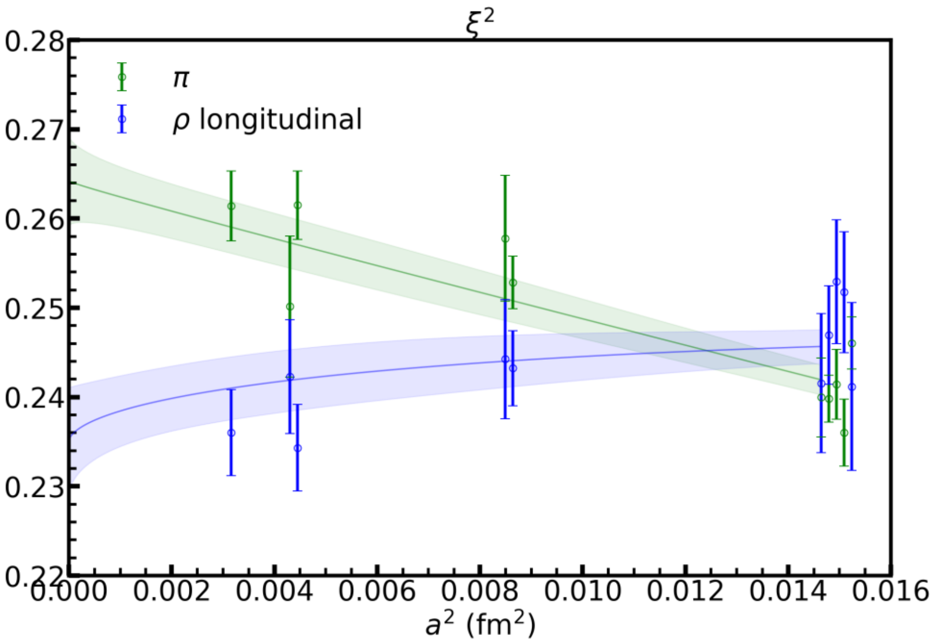

The lattice spacing dependence, Every data points have corrected to physical mass.

Chiral behavior of second moments

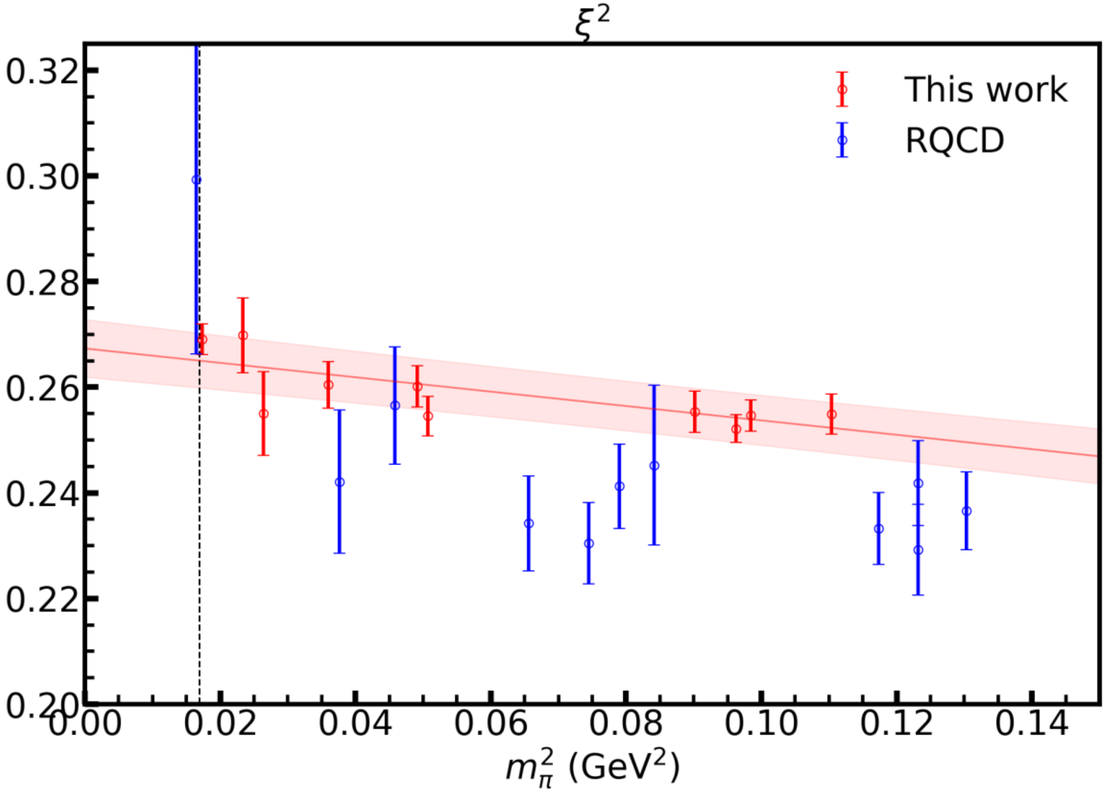

	$a_\pi^{(2)}$	$a_K^{(1)}$	$a_K^{(2)}$	
RBC/UKQCD [22]	0.23(3)(6)	0.036(1)(2)	0.18(3)(6)	
RQCD [24]	0.116^{+19}_{-20}	0.0525^{+31}_{-33}	0.106^{+15}_{-16}	
This work	0.187(15)	0.0481(23)	0.158(14)	
	$a_\rho^{(2)}$	$a_{K*}^{(1)}$	$a_{K*}^{(2)}$	$a_\phi^{(2)}$
RBC/UKQCD [22]	0.20(3)(6)	0.037(1)(2)	0.15(6)(6)	0.15(6)(3)
RQCD [25]	0.132(27)			
This work	0.102(18)	0.0609(15)	0.085(17)	0.069(17)

The deviation between our results and those of RQCD is larger than 2σ.

The error of the RQCD result is very large at the physical pion mass, and its central value deviates from the fit line. However, when considering results with $m_\pi^2 < 0.05\ \mathrm{GeV}^2$, they are consistent, and those with $m_\pi^2 < 0.10\ \mathrm{GeV}^2$, still within 2σ. Our work includes more data points close to the physical pion mass and has better signal quality. Therefore, the deviation may come from an underestimation of the effects from results near the physical pion mass.

Extrapolation for first moments

The global fit ansatz :

$$\langle\xi\rangle_M(m_{\pi,\eta_s}^{\text{v,sea}}, a, 1/L) = \langle\xi\rangle_M^{\text{phys}}[1+\delta(c_{1/2,M}^{(1)}, a, 1/L)][(1-c_{3,M}^{(1)})\delta m_q^{\text{v}} + c_{3,M}^{(1)}\delta m_q^{\text{sea}}]/\delta m_q^{\text{phys}},$$

Where $\delta(c_{1/2/3}, a, 1/L) = c_1\bar{\alpha}_s\Lambda_\chi a + c_2\Lambda_\chi^2 a^2$, $\bar{\alpha}_s \equiv -\frac{4}{3}\ln u_0$ and $\Lambda_\chi = 1\,\text{GeV}$

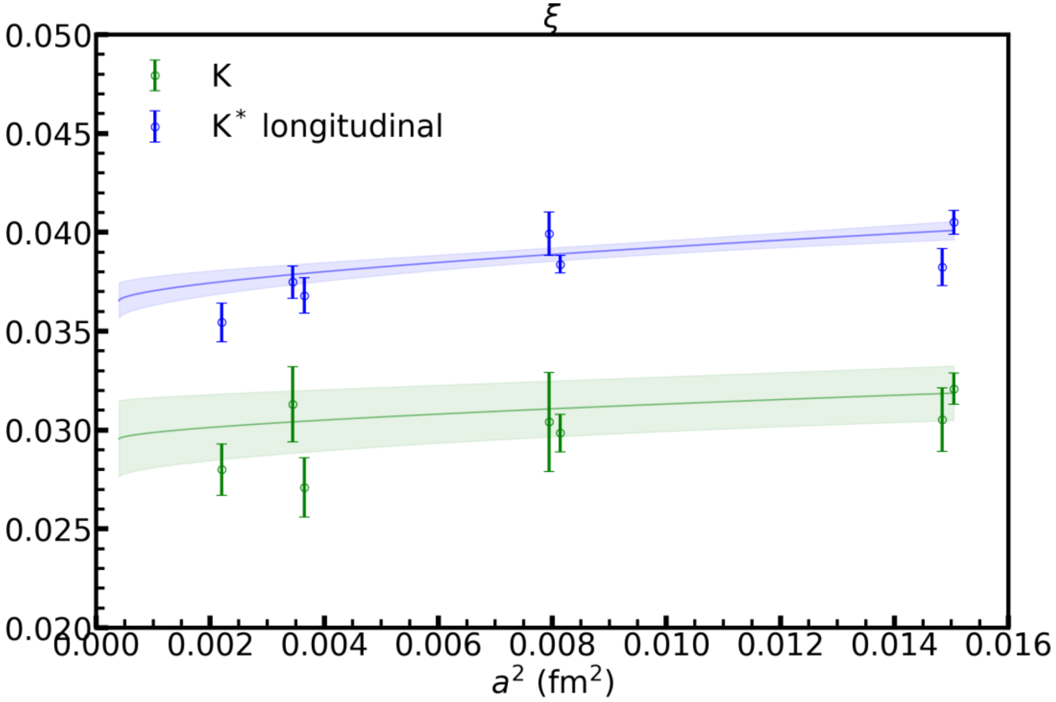

The lattice spacing dependence, Every data points have corrected to physical mass.

Chiral behavior of first moments

The first moments should be proportional to the $m_s - m_l$. In figure, every data points have corrected to unitary point.

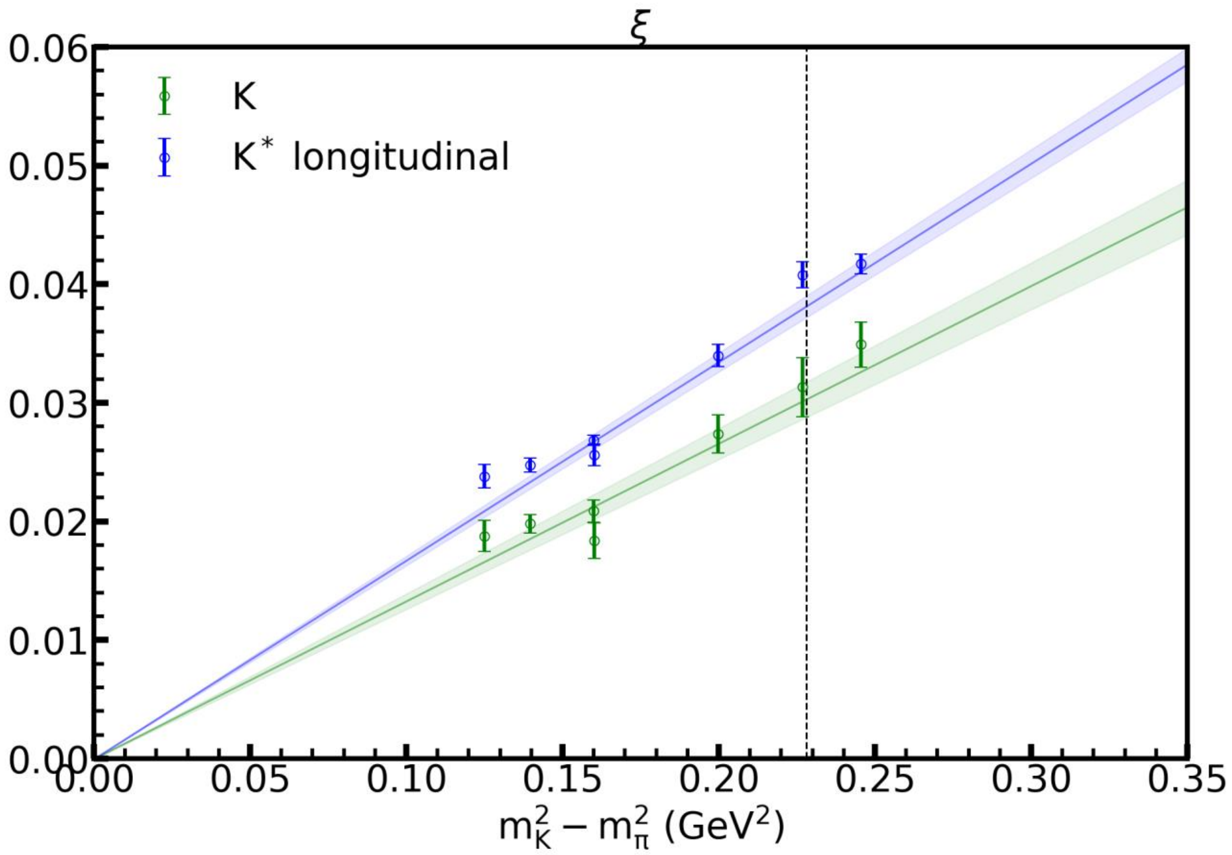

	$a_\pi^{(2)}$	$a_K^{(1)}$	$a_K^{(2)}$	
RBC/UKQCD [22]	0.23(3)(6)	0.036(1)(2)	0.18(3)(6)	
RQCD [24]	0.116^{+19}_{-20}	0.0525^{+31}_{-33}	0.106^{+15}_{-16}	
This work	0.187(15)	0.0481(23)	0.158(14)	
	$a_\rho^{(2)}$	$a_{K^*}^{(1)}$	$a_{K^*}^{(2)}$	$a_\phi^{(2)}$
RBC/UKQCD [22]	0.20(3)(6)	0.037(1)(2)	0.15(6)(6)	0.15(6)(3)
RQCD [25]	0.132(27)			
This work	0.102(18)	0.0609(15)	0.085(17)	0.069(17)

Our result for the first moment is consistent with that of RQCD.

Moments from Non-local operator

Using LaMET, we can obtain the LCDA in coordinate space,

$$H_m^{\rm R}(\lambda, P_z) = \int_0^{\lambda} d\lambda' \, M(\lambda, \lambda', \mu) h_m(\lambda', P_z)$$

Where $H(z, P_z) = \langle \Omega | \bar{q}_2(-z/2) e^{i\int_{-z/2}^{z/2} gA_z(xn_z)dx} n\gamma_5 q_1(z/2) | M(P_z) \rangle$

and $H_m^R(z, P_z) = \dfrac{H_m^B(z, P_z)}{Z_{\rm self}(a, z) H_m^{\overline{\rm MS},\ 1-{\rm loop}}(z)}$.

The moments correspond to derivatives of the LCDA in this space.

$$e^{-i\lambda/2} h_m(\lambda) = \sum_{n=0}^{\infty} \left(\frac{-i\lambda/2}{n!}\right)^n \langle \xi^n \rangle$$

By applying this relation, we obtain the second moments, which are consistent with those extracted from local operators after extrapolation.

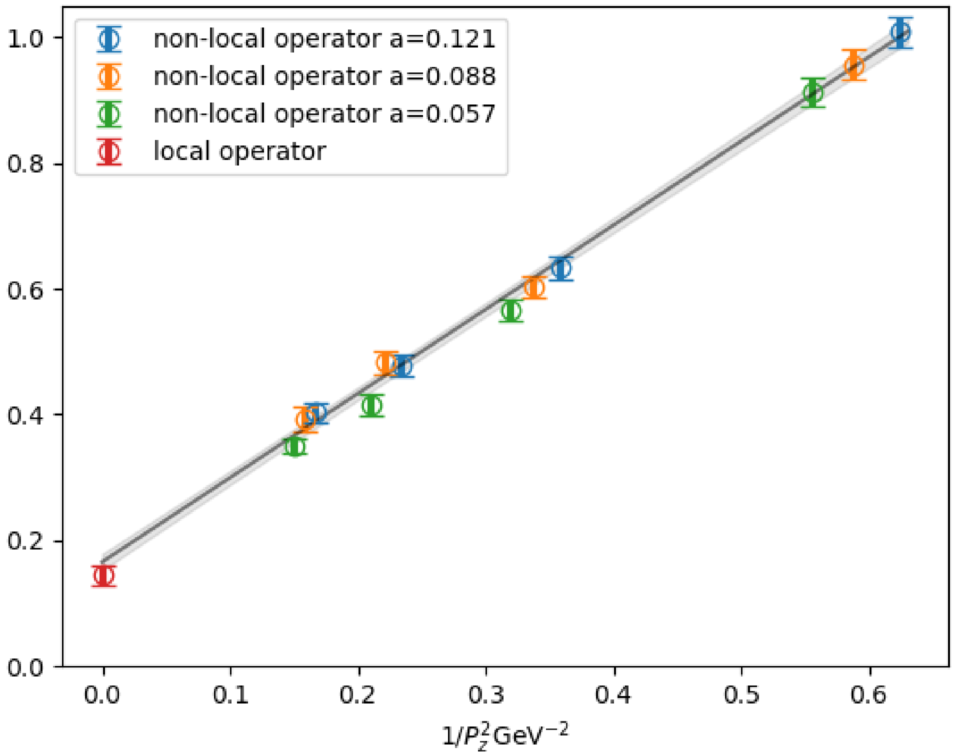

The second moments of kaon

The puzzle of first moments

In previous work, The first moments of the LCDA for pseudoscalar mesons and the transverse components of vector mesons have a sign opposite to that of the longitudinal components of vector mesons.

These are the pseudoscalar Quasi-DAs obtained using different source and sink operators on a09m310. As shown, the sink operator $\gamma_t\gamma_5$ yields a result with sign opposite to that of $\gamma_z\gamma_5$. We have verified that the sign from the $\gamma_t\gamma_5$ sink is correct.

$\mathrm{Im}[h(\lambda)]$

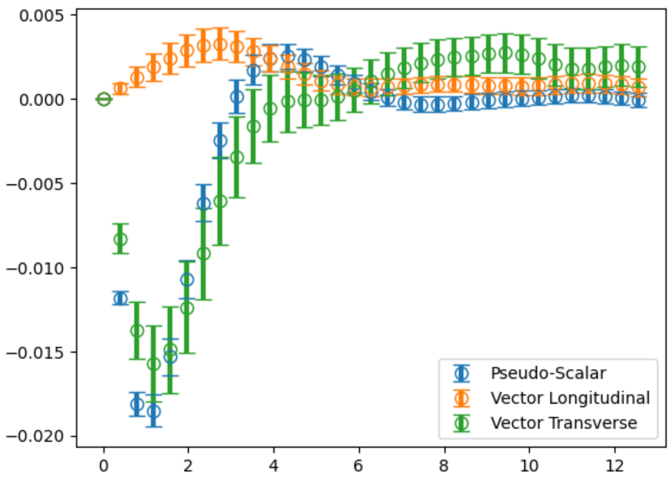

$\mathrm{Im}[H(z)]$

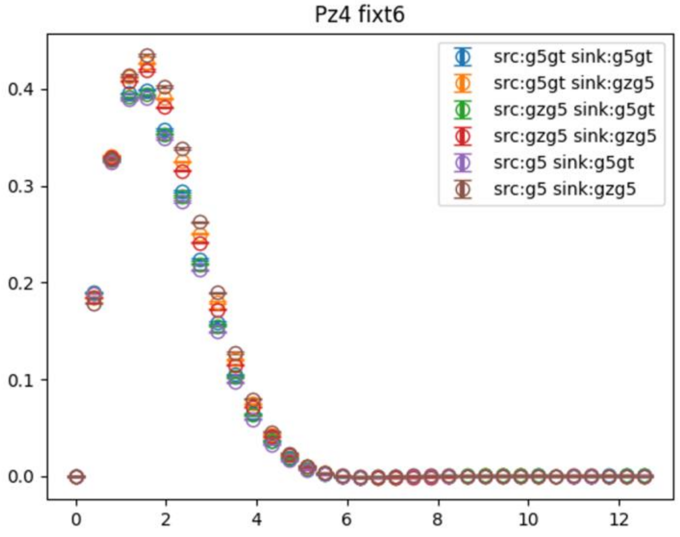

$\mathrm{Im}[e^{-izP_z/2}H(z)]$

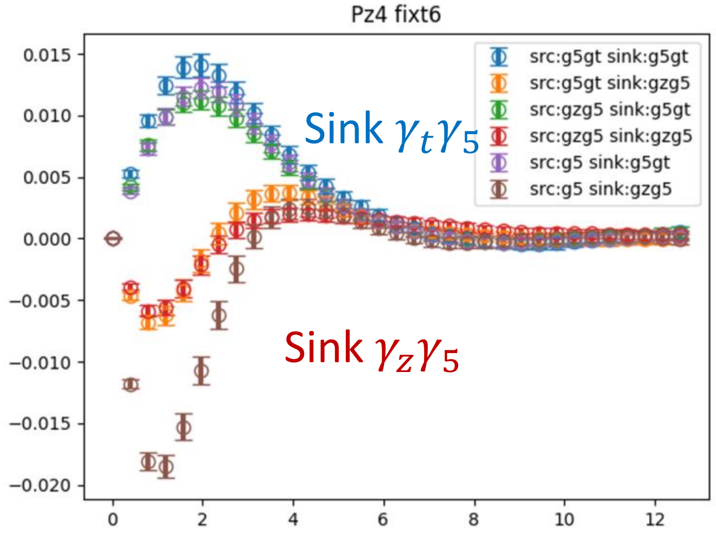

The higher-twist and excited state contamination

These are the momentum dependence of pseudoscalar Quasi-DAs of different channel

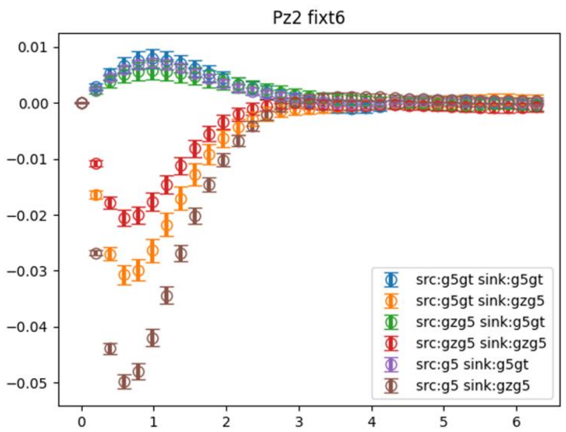

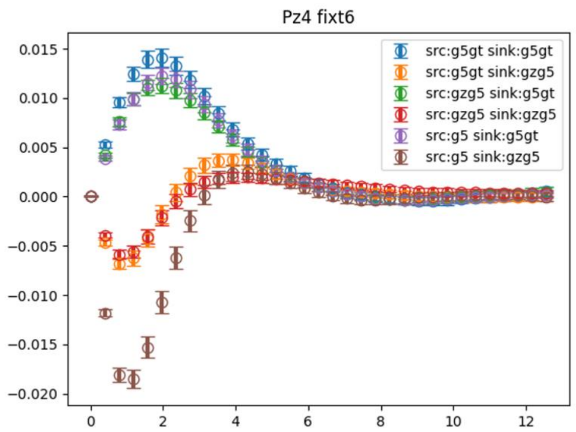

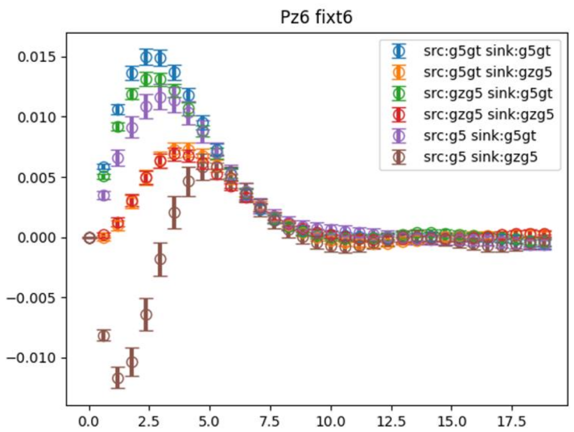

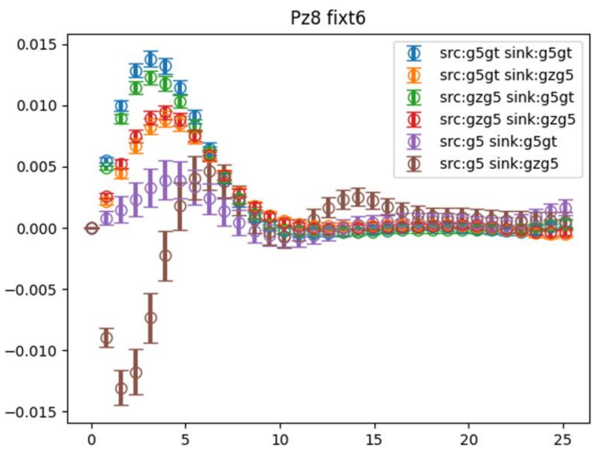

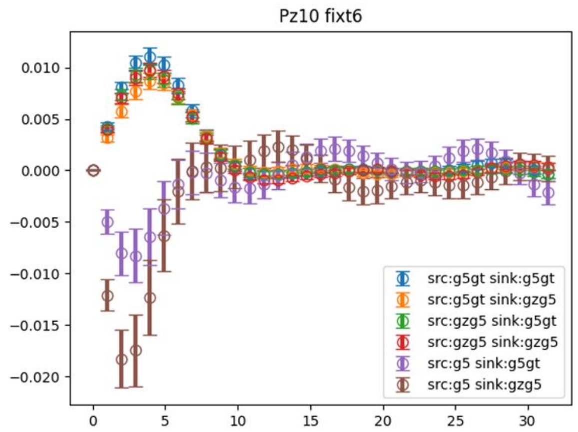

$$\langle \Omega | \gamma_\mu \gamma_5 D_\nu | M(p) \rangle = a\left(p_\mu p_\mu - \frac{1}{4} g_{\mu\nu}\right) + b g_{\mu\nu}$$

The first derivative of the $\gamma_t\gamma_5$ quasi-DA correlator contains only the first term.

For the sink operator $\gamma_z\gamma_5$, both the $\gamma_z\gamma_5$ and $\gamma_t\gamma_5$ sources approach the correct sign as momentum increases. However, the γ_5 source remains negative.

For the sink $\gamma_t\gamma_5$, the γ_5 source surprisingly becomes negative at high momentum. Since the $\gamma_t\gamma_5$ sink is free of higher-twist contamination, this sign change must originate from **excited-state contamination**.

The higher-twist and excited state contamination

source: γ_5 sink: $\gamma_z\gamma_5$ source: γ_5 sink: $\gamma_t\gamma_5$

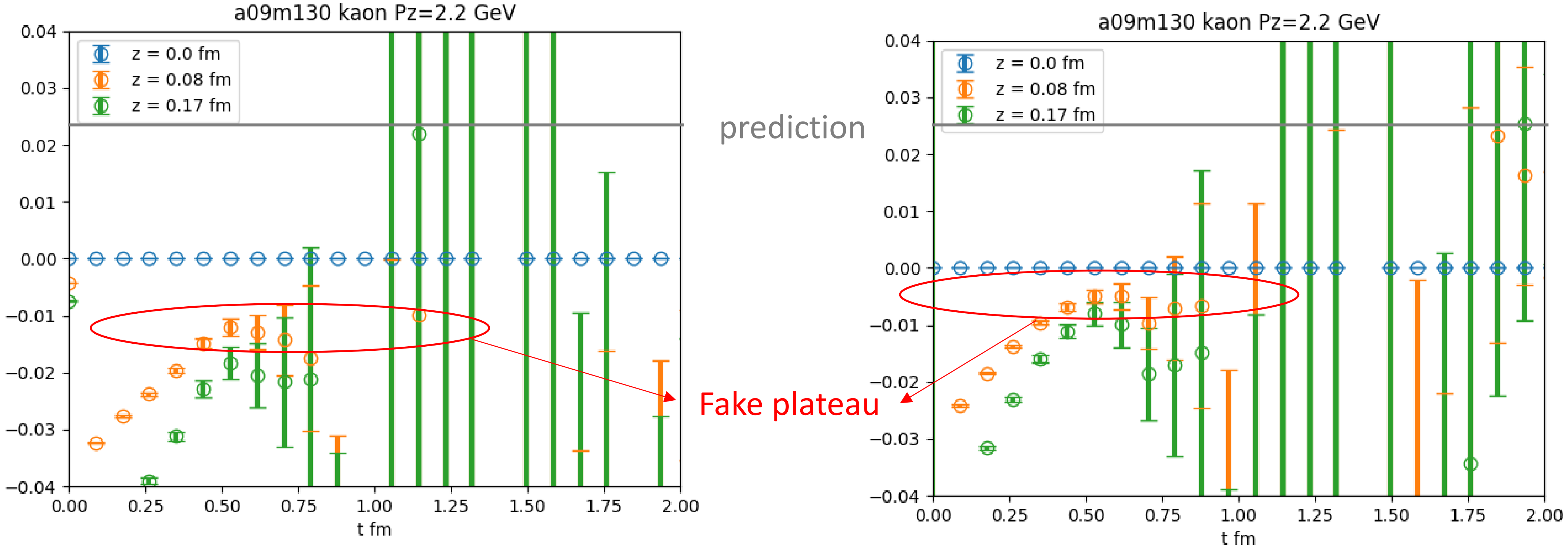

When the source operator is γ_5, the fit easily converges to a fake plateau, which remains far from the true plateau.

Therefore, using γ_5 as the source operator is problematic for reliably extracting the correct DA. Using source operator as $\gamma_t\gamma_5$ and $\gamma_z\gamma_5$ are better choices.

The higher-twist and excited state contamination

For vector meson, the cases are similar

transverse components of vector mesons

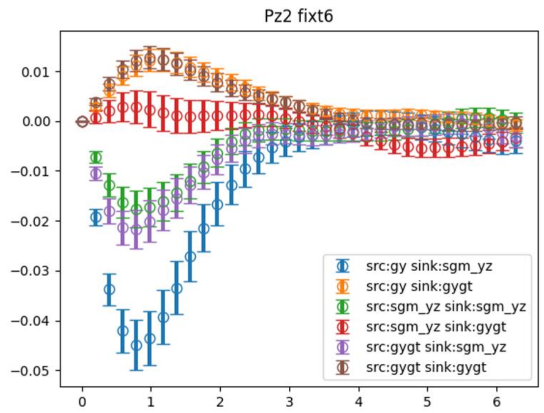

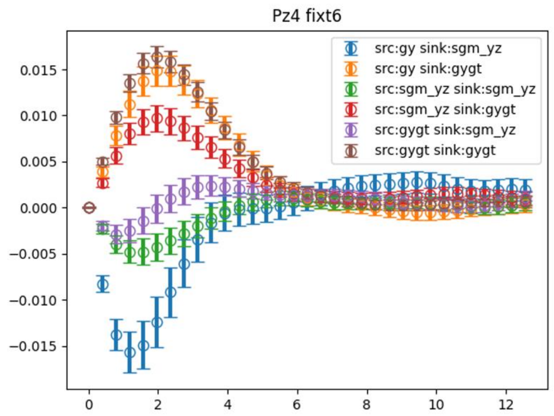

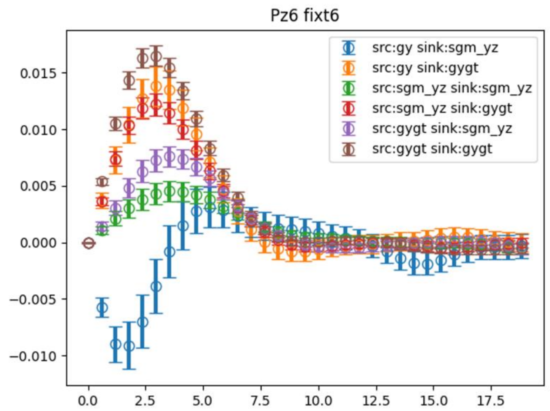

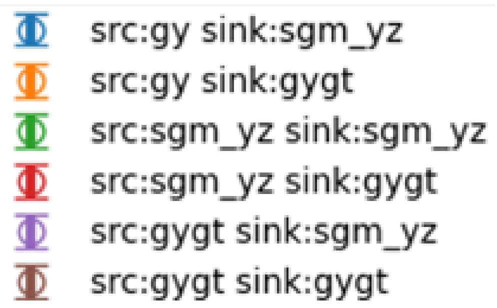

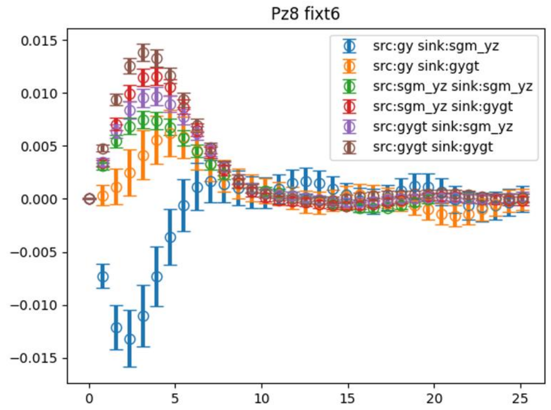

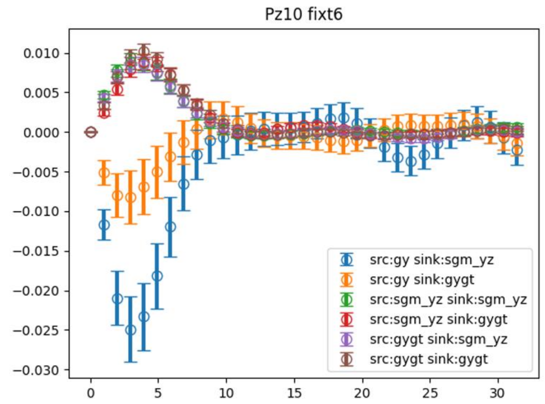

For the sink operator σ_{yz}, both the σ_{yz} and $\gamma_y\gamma_t$ sources approach the correct sign as momentum increases. However, the γ_y source remains negative.

For the sink $\gamma_y\gamma_t$, the γ_y source becomes negative at high momentum.

The higher-twist and excited state contamination

longitudinal components of vector mesons

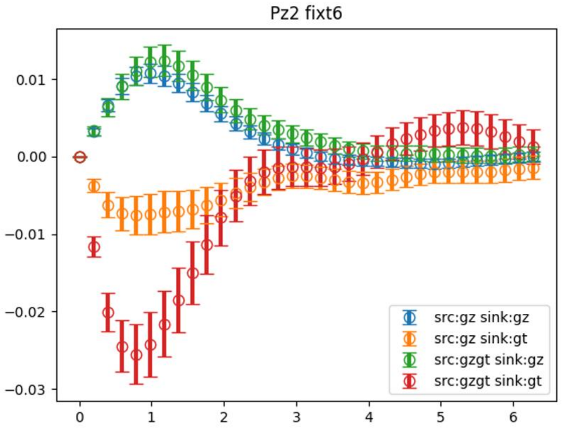

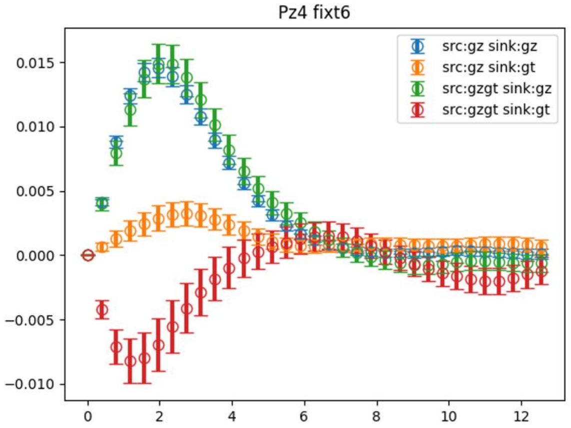

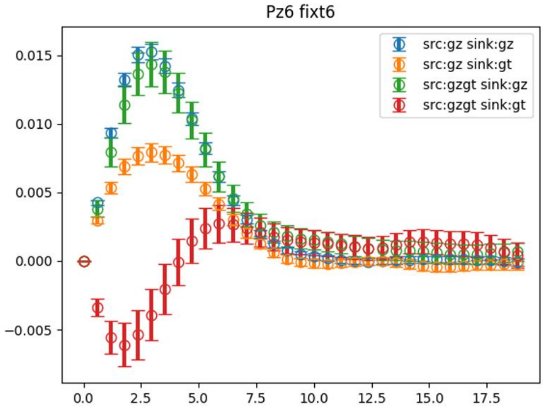

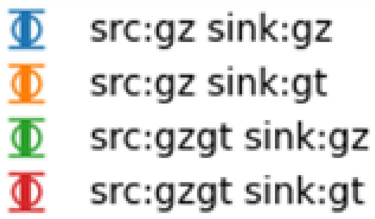

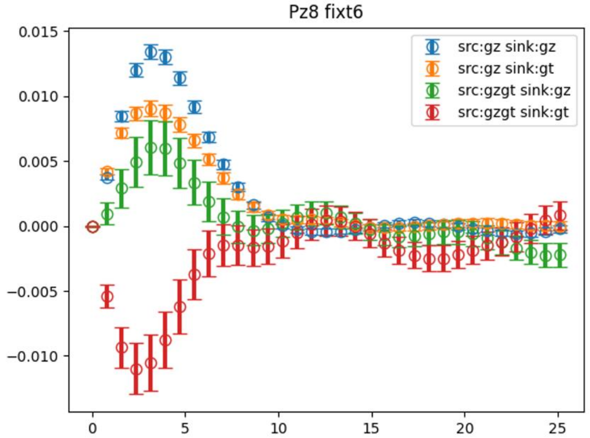

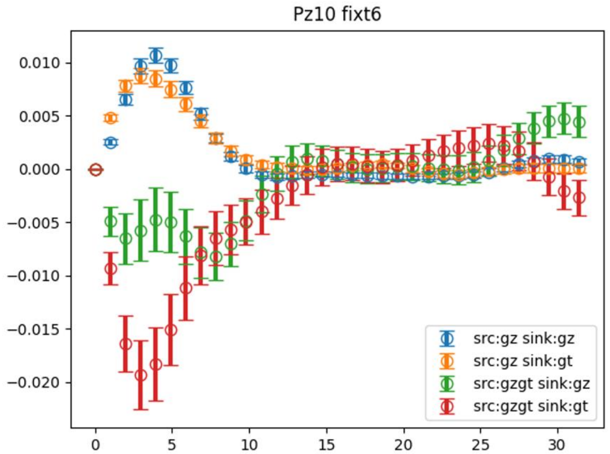

For the sink operator γ_t, γ_z sources approach the correct sign as momentum increases. However, the $\gamma_z\gamma_t$ source remains negative.

For the sink γ_z, the $\gamma_z\gamma_t$source becomes negative at high momentum.

The higher-twist and excited state contamination

The next problem is the magnitude of the first moments is still smaller than the predict even process the right sign. This can also be seen in $\gamma_t\gamma_5$ channel.

The first moments extract from local traceless operator and non-local operator of different P_z

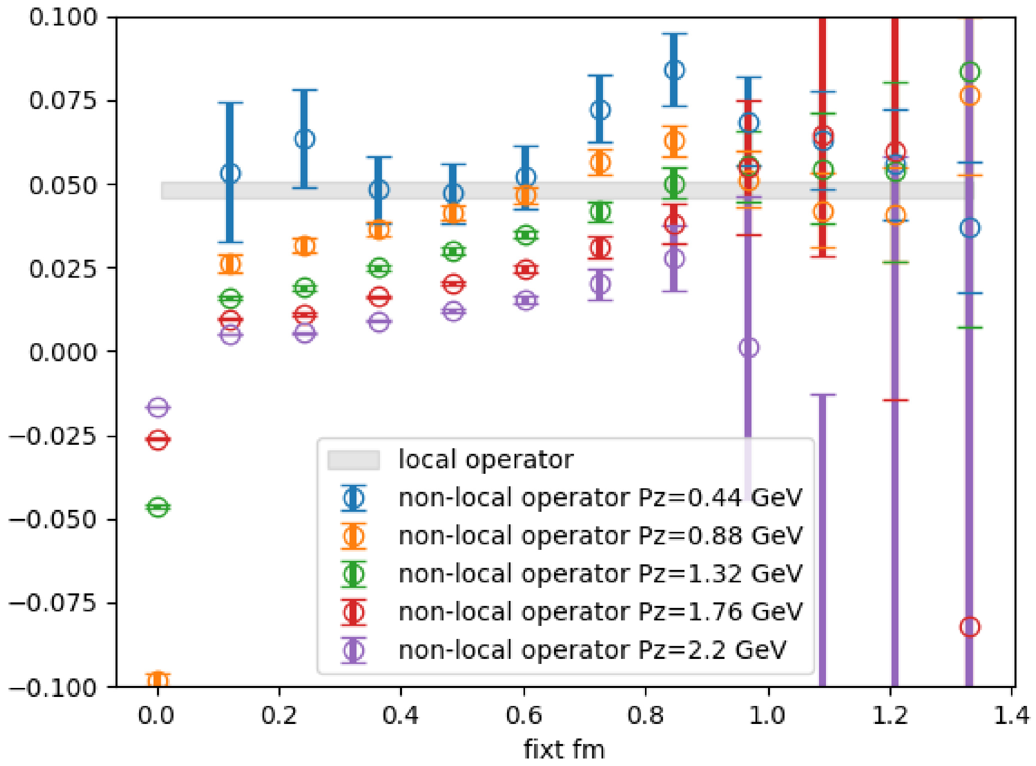

non-local operator source: $\gamma_t\gamma_5$ sink: $\gamma_t\gamma_5$

Since the sink operator $\gamma_t\gamma_5$ is free of higher-twist contamination, this decline with increasing momentum must originate from **excited-state contamination**.

The most important thing is:
control the contamination of excited states.

Summary

- Based on the twist-2 local operator, we obtain highly precise values for the meson LCDA moments at the physical point and in the continuum limit.

- The higher-twist contributions can be effectively suppressed at large momentum. The wrong sign and small magnitude both come from excited-state contamination. It is important to suppress excited-state contamination to obtain accurate DA.